



Utilizing Industrial Fennel Seed Waste and Brilliant Green from Nutraceuticals for a Sustainable Wastewater Dye Adsorption System

Razia Sulthana¹, H C Basavaraju², Syed Noeman Taqui², H N Deepakumari³,
Rayees Afzal Mir⁴, Akheel Ahmed Syed^{5*}, Khalid Ansari^{6**}, Shareefraza J. Ukkund⁷,
Majed Alsubih⁸, Saiful Islam⁸

¹Department of Studies in Chemistry, University of Mysore, Manasa Gangothi, Mysuru, India

²Department of Studies in Chemistry, Bharathi College – Post Graduate and Research Centre,
Bharathi Nagara, Karnataka, India

³Department of Chemistry, Regional Institute of Education, Bhubaneswar, Odisha, India

⁴Glocal School of Agricultural Science, Glocal University, Mirzapur pole, Saharanpur, Uttar Pradesh, India

⁵Centre for Advanced Research and Innovation, Glocal University, Delhi-Yamunotri Marg, Mirzapur Pole,
Saharanpur District, Uttar Pradesh, India

⁶Department of Civil Engineering, Yeshwantrao Chavan College of Engineering, Nagpur, Maharashtra, India

⁷Department of Biotechnology, P. A. College of Engineering, Mangaluru, India

⁸Civil Engineering Department, College of Engineering, King Khalid University, Abha, Saudi Arabia

*corresponding author's e-mail: akheelahmed54@gmail.com

**corresponding author's e-mail: ksansari@yuce.edu

Abstract: The possibility of using nutraceutical fennel seed spent (NIFSS) as an affordable biosorbent to extract brilliant green (BG) from aqueous solutions. Various factors were examined to assess their impact on the adsorption route. Several isotherm models were recycled to assess experimental equilibrium data. The Brouers–Sotolongo isotherm model demonstrated a maximum adsorption ability. The pseudo-second order model provided an exceptional fit. The adsorption practice was both spontaneous and endothermic. Potential interactions occurring in the BG-NIFSS system were discussed. Overall, this investigation highlights NIFSS as an effective and reasonably priced biosorbent for removing dangerous BG from water-based systems.

Keywords: nutraceutical industrial fennel seed spent, brilliant green, kinetics, modelling, thermodynamics

1. Introduction

Environmental pollution, particularly in aquatic environments, threatens all living organisms significantly (Nandi et al. 2009). Textiles, pulp and paper, paint, and leather industries employ many dyes and pigments in their manufacturing processes. Textile industries, in particular, consume substantial amounts of water and organic chemicals for colouring purposes (Waghmare et al. 2023). When this coloured wastewater discharges into ecosystems, it contributes to aesthetic pollution and disrupts aquatic life. Coloured waste in rivers and streams hinders sunlight penetration, subsequently reducing photosynthesis (Namasivayam 2001, Gupta et al. 2022). Synthetic dyes are extensively used in industries like paper, textiles, food, and pharmaceuticals. Unfortunately, due to improper processing and dyeing methods, around 40,000-50,000 tons of these dyes continuously enter water systems. These dyes possess aromatic structures that make them exceedingly stable and deterioration-resistant (Waghmare et al. 2024). The primary contributors to dye consumption are textile dyes. A 12% or more loss of synthetic dyes occurs during production and processing, and 20% find their way into industrial wastewater (Filipkowska et al. 2002). Moreover, these dyes have been identified as carcinogenic, mutagenic, or teratogenic to various microorganisms. They can also inflict severe harm on human health, leading to kidney dysfunction, reproductive issues, liver problems, and damage to the brain and central nervous system (Kadirvelu et al. 2003). Over 10,000 distinct compounds comprise more than 7×10^5 tons of dyes and pigments shaped yearly globally (Zollinger 2002). Therefore, removing these colours from textile effluents is crucial before releasing them into natural water bodies.

Brilliant green (BG) is a hazardous cationic dye containing triphenyl nitrogen. It finds application in various manufacturing sectors, such as paper, green ink, and textiles. However, BG dye is known to be toxic, mutagenic, and carcinogenic, posing risks to aquatic life and humans (Bhattacharyya & Sarma 2003). One particularly concerning effect is its potential to produce eye burns, which could lead to long-term harm to people's and animals' eyes (Mittal et al. 2008). BG dye is utilised per ton of paper produced in the paper industry, and 0.8-1.0 kilograms of BG are consumed. Unfortunately, exposure to BG can cause intestinal irritation



in humans, which can result in symptoms including both diarrhoea and vomiting. Additionally, it might irritate the respiratory system, causing coughing and shortness of breath (Mane et al. 2007).

The efficacy has been highlighted by numerous research published in the literature on colour removal methods, with adsorption emerging as the most economically viable and commonly employed technique. A growing number are interested in utilising easily accessible, affordable adsorbents for this purpose, as indicated by research by Salman and Hameed (2010) and Garg et al. (2003). But because regeneration is expensive and complicated, scientists have been looking for cheaper alternatives to adsorbents for a while now. Consequently, eliminating colour from wastewater remains a significant environmental challenge confronting our society. In addressing this issue, the adsorption process is an attractive alternative and highly effective wastewater treatment and management method.

The Nutraceutical Industry, which falls under the agro-industrial sector, is experiencing significant growth. Following the research "Emerging Indian Nutraceutical Market" touched 6.1 billion US\$ by the year 2020 (www.ibef.org). However, a significant challenge this industry faces pertains to waste management, which accounts for a substantial portion of the total waste. To extract the active ingredient(s), the volume of managed herbs, shrubs, seeds, and/or roots ranges from 50% to 95%.

Fennel, scientifically known as *Foeniculum vulgare*, is an herbaceous herb belonging to the Umbelliferae family. It can grow up to 2 meters in height. India is the leading manufacturer of fennel seeds, churning out a whopping 11×10^4 tons annually. Fennel seeds are notably rich in dietary fibre, containing approximately 1-3% impulsive oil (www.spices.res.in). The critical nutrients in fennel include vitamins, minerals, essential oils, fibre, protein, and antioxidants. These components are necessary for protecting against oxidative stress-related harm and enhancing the immune system. However, a substantial amount of waste, known as spent, is generated during the industrial processes involved in extracting principal components from fennel seed production. This spent has undergone thermal, mechanical, and chemical treatments, rendering it devoid of commercial, feed, or fertiliser value. In the present study, this fennel seed spent, referred to as Nutraceutical Industrial Fennel Seed Spent (NIFSS), has been repurposed in a readily usable form for efficient adsorption of Brilliant Green (BG) from aqueous solutions. This research investigates the adsorption capacity of NIFSS, which is renewable, cost-effective, and abundantly available, owing to its unique pore structure that enhances its adsorption capabilities.

To effectively manage the substantial volume of wastewater and textile effluent produced by the textile industry, Nutraceutical Industrial Spent (NIS), available in abundant quantities, appears to be a viable solution. What sets NIS apart is its unique set of properties that other adsorbents have not been reported. Before being discarded as used in the business, nutritional supplements undergo heat, mechanical, and chemical processing to extract their essential ingredients. Therefore, Brilliant Green (BG) from water or industrial effluents can be remedied with NIS without requiring extra chemical treatment. This property benefits from lowering the E-factor (Sheldon 1992). Furthermore, the fibril structure of NIFSS can capture moisture content, cause a decline in calorific value, and cause a rise in harmful emissions. It's interesting to note that this same ability can be used to improve the sorption of harmful dyes onto NIFSS.

The objective of the existing study is to ascertain whether NIFSS, a by-product from the nutraceutical industry, can be employed as a biosorbent that effectively and affordably removes harmful BG dye from aqueous solutions.

2. Materials and Methods

2.1. Adsorbate

Brilliant Green (BG) was sourced from Sigma Aldrich Private Ltd, Mumbai, India. Double-distilled water was used to dissolve the dye in precisely the right amounts to prepare BG solutions for experimentation.

2.2. Preparation of adsorbent

The local industry provided the Nutraceutical Industrial Fennel Seed Spent (NIFSS) used in this investigation. The following steps were followed to prepare it for use in the research:

1. Drying: The NIFSS was dried for 24 hours at 60°C in an oven.
2. Grinding: The time spent after drying, the material was finely ground to a powder-like consistency.
3. Sieving: The ground material was obtained from particles smaller than $\leq 177 \mu\text{m}$ after being sieved with an ASTM 80 mesh sieve.
4. Storage: Finally, plastic containers were used to store the processed NIFSS for later use. Notably, the substrate underwent no extra physical or chemical changes before being used in the adsorption process. This procedure outlines the preparation of NIFSS for its role as an adsorbent in the research, ensuring its suitability for the intended purpose.

2.3. Characterisation of spent

This study scrutinised Nutraceutical Industrial Fennel Seed Spent (NIFSS) morphology using a Zeiss scanning electron microscope, specifically the Evo/LS15 model. Fourier-transform infrared Spectroscopy (FTIR) was employed to analyse the functional groups in the dye-adsorbed and unadsorbed materials. A Perkin Elmer Spectrophotometer equipped with FTIR capabilities was utilised for the FTIR analysis. The spectral analysis covered a range of 400 to 4000 cm^{-1} . By equating the FTIR spectra of the adsorbed and unadsorbed spent materials, insights into the changes in functional groups due to the adsorption process could be obtained. These analytical techniques provide valuable information about the structural and chemical characteristics of NIFSS and how they are affected by the adsorption of target substances of the adsorption method.

3. Results and Discussion

3.1. Exterior description of spent

3.1.1. Scanning electron microscopy

As shown in Fig. 1a, the NIFSS SEM examination indicated a fibrous and porous structure (Haris & Sathasivam 2009). This particular building plays a crucial role in facilitating dye adsorption. In Fig. 1b, you can observe the pores and empty spaces filled with the dye.

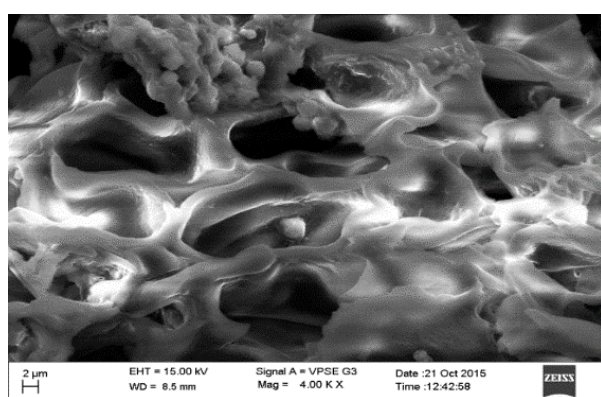


Fig. 1a. NIFSS earlier adsorption

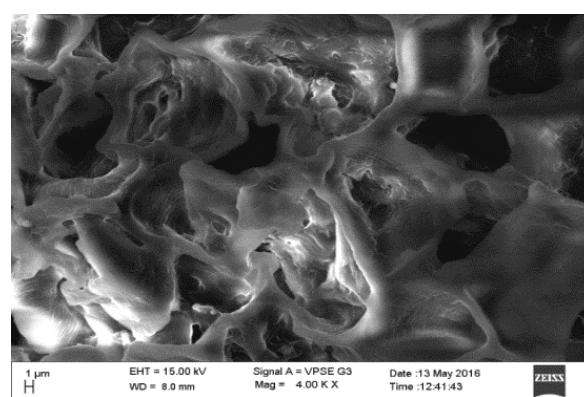


Fig. 1b. NIFSS later adsorption

3.1.2. FTIR Spectroscopy

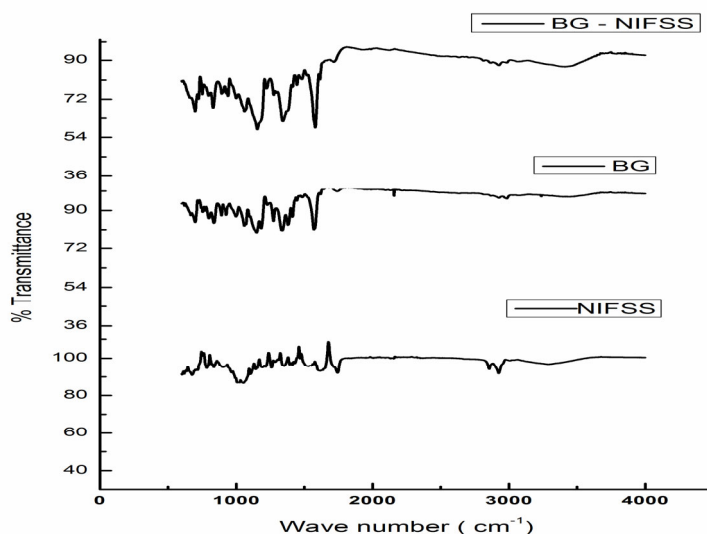


Fig. 2. FTIR spectra

As shown in Fig. 2, the spectral study provided valuable information regarding chemical interactions during adsorption. Here's a breakdown of the key findings from the FTIR analysis:

- C=C stretching in olefins was identified by a band at 1742 cm^{-1} , whereas a band indicated the occurrence of methyl groups at 1411 cm^{-1} .
- A wide band around 3284 cm^{-1} was identified, credited to surface hydroxyl groups, typically joined in cellulose, and absorbed water bands at 2925 cm^{-1} , indicating stretching vibrations in the -CH bonds of alkane and alkyl groups. The band is 1056 cm^{-1} in the suggested size of the adsorbent that included cellulose.
- Following the adsorption process shifts in certain bands were observed. For instance, the shift from 2925 to 2967 cm^{-1} confirmed the involvement of BG. The band at 2881 cm^{-1} in alkane and alkyl groups having carbon and hydrogen is linked to the stretching vibrations of the -CH bonds, further supporting the interaction of BG during adsorption.
- Notably, a decrease in occurrence from 1569 cm^{-1} to 1467 cm^{-1} was observed, attributed to stretch vibrations of C=C bonds in the quinoid structure assembly of BG.
- The dye molecule's C-N stretching and C-H distortion were responsible for the bands at 1467 cm^{-1} and 1385 cm^{-1} , respectively, and they did not undergo any substantial post-adsorption changes.
- The analysis revealed shifts in specific peaks, some disappearance, and new peaks' appearance. These spectral changes showed the participation of particular functional groups in the adsorption method.
- Importantly, absorption groups of 1000 cm^{-1} and 800 cm^{-1} were detected, indicating changes in the chemical transformation. This FTIR spectroscopy technique allowed for identifying adsorbent and adsorbate groups responsible for the dye adsorption process.

In conclusion, the FTIR analysis offered insightful information about the chemical transformations and interactions occurring during the dye's adsorption, shedding light on the mechanisms and including functional groups in the method.

3.2. Batch adsorption studies

3.2.1. Result of initial dye concentration and contact time

Taking up of the dye exhibited an increase, reaching up to 150 mg g^{-1} for pepper seed spent, when the solution's initial dye concentration improved from 25 to 300 mg L^{-1} . The higher driving force caused by the gradient of concentrations that develops as the initial dye concentration grows can be used to explain these phenomena. Fig. 3a illustrates the uptake of Brilliant Green (BG) over time, and it's evident that the uptake rises with longer contact times. The longest period of BG removal from the aqueous solution during contact time was achieved after 180 minutes. The subsequent, relatively delayed process for dye molecules to permeate holes (interior surface) caused the process to slow down.

The adsorption of BG continued to increase with increasing concentration until it reached a plateau after reaching equilibrium. At this point, the biosorption rates levelled off to a constant value as all available adsorption sites became occupied, leaving no active sites for further binding of dye molecules to the biosorbent's surface. Early on, there are a lot of open surface areas that are suitable for adsorption. The remaining open surface areas are still available for use, but it becomes more progressively challenging because of the antagonistic interactions that arise between the bulk and solid phases of solute molecules. This behaviour is consistent with prior research findings (Nandi et al. 2009a, Asadullah et al. 2010).

In summary, the uptake of BG was influenced by both initial concentration and contact time, with adsorption being most effective when equilibrium was achieved and all available adsorption sites were utilised.

3.2.2. Outcome of adsorbent dosage

The significant aspect inspected in the batch tests was the effect of the adsorbent dose. This parameter was studied within the series of 0.025 to 0.2 g. As depicted in Fig. 3b, the results clearly illustrate that the yield of BG adsorption onto NIFSS increased as the adsorbent dosage was elevated. This effect is brought about by the larger adsorbent's increased surface area and better adsorption site disposal. Nevertheless, it's interesting to observe that further increases in the adsorbent dose had no discernible impact on the adsorption yield. Since almost all of the dye molecules are attached, a balance among the molecules of the adsorbent surface is established for the dye in the solution and on the adsorbent. This observation aligns with previous research findings (Hiroyuki et al. 1994).

In summary, the dye's sorption directly correlated with the adsorbent dosage, reaching an equilibrium value after a certain level of adsorbent dosage was attained. Beyond this point, additional adsorbent did not significantly enhance the adsorption yield.

3.2.3. Outcome of temperature

Every adsorption process is influenced by temperature, and in this study, adsorption studies were executed in the 30°C to 50°C range, with the results depicted in Fig. 3c. Notably, higher temperatures accelerated the adsorption rate. This discovery is explicable given that greater temperatures promote the ions in the solution moving thermally, which raises the adsorbent's capacity. Additionally, a rise in temperature accelerates the pace at which adsorbate molecules move through the adsorbent's external border level. It was fascinating to observe that when the temperature rose, the adsorption capability fell and also showed a modest rise. The adsorption process may be exothermic, according to this indication. In summary, the study indicates that higher temperatures enhance the adsorption rate by increasing thermal motion and mass transfer, and it also suggests that the adsorption process releases heat, classifying it as exothermic.

3.2.4. Outcome of pH

A solution's pH significantly impacts the adsorbent's outward charge and the ionisation state of the chemicals in it. It is regarded as one of the most crucial adsorption process parameters because it directly affects adsorption capacity, external characteristics of the adsorbent, and the development of ionic dye in the mixture. The pH value also has consequences for the structural stability of Brilliant Green (BG). Notably, BG solution exhibits stability within the initial pH range of 3 to 4. However, deviations from this range, whether towards higher or lower pH values, cause the ability for adsorption to decline. At a pH level of 9, the BG solution begins to decolourise spontaneously, and at even higher pH values, instability in the solution causes turbidity and, eventually, precipitation. This instability of BG in response to changes in pH alone may be attributed to structural alterations occurring within BG molecules, as depicted in Fig. 3d (Sudamalla et al. 2012). In conclusion, the pH of the solution affects both the dye solution's stability and the adsorbent's surface characteristics, which is particularly significant given the changes to the BG molecule's structures.

3.2.5. Outcome of particle size

The results, as illustrated in Fig. 3e, reveal that a fall in the proportion of dye removal results from a decrease in dye adsorption as particle size increases. Because smaller particles have more surface area accessible for adsorption, this phenomenon can be explained. Larger particles, on the other hand, possess more excellent mass transfer diffusion resistance, and most of the inner surface might not be efficiently utilised for adsorption. As a result, in the case of bigger particles, the quantity of dye adsorbed is decreased (Wang et al. 2006). In conclusion, particle size affects adsorption significantly, with smaller particles offering a greater surface area and better adsorption capacity. In comparison, larger particles exhibit decreased adsorption due to higher mass transfer resistance.

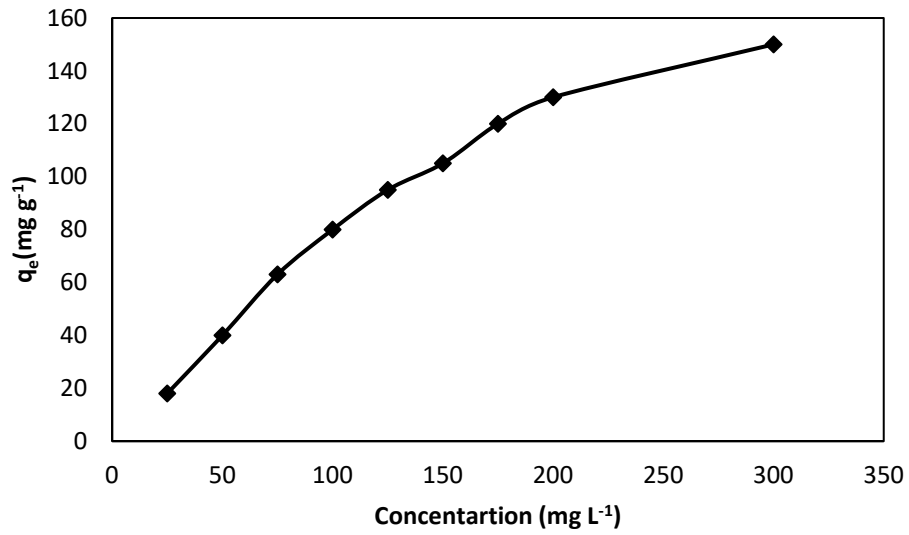


Fig. 3a. Outcome of initial concentration

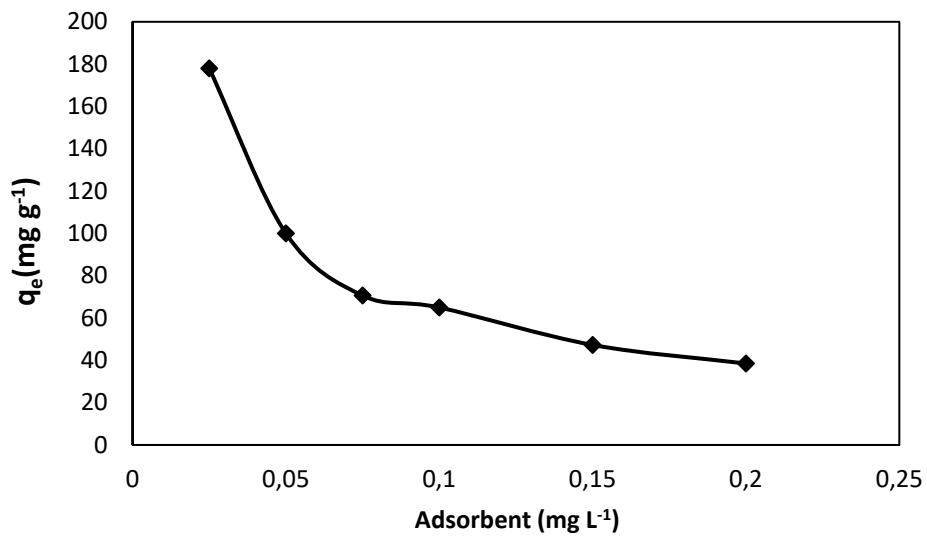


Fig. 3b. Outcome of adsorbent dosage

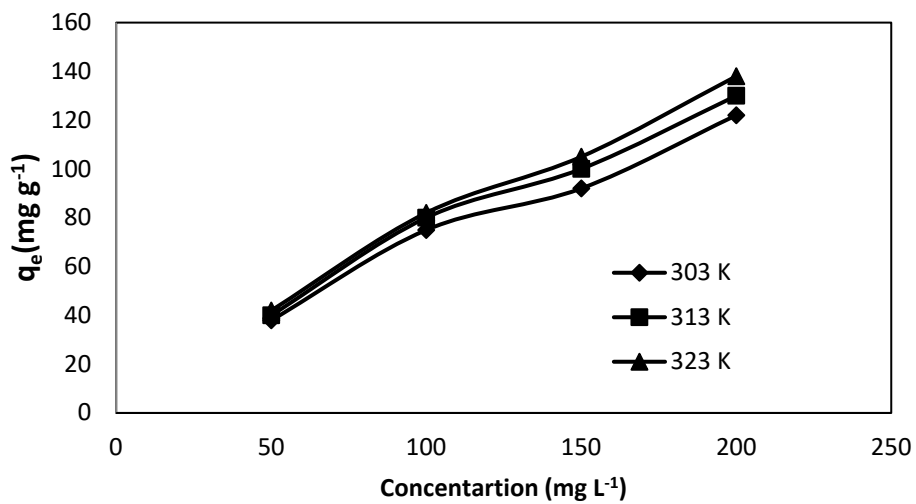


Fig. 3c. Outcome of temperature

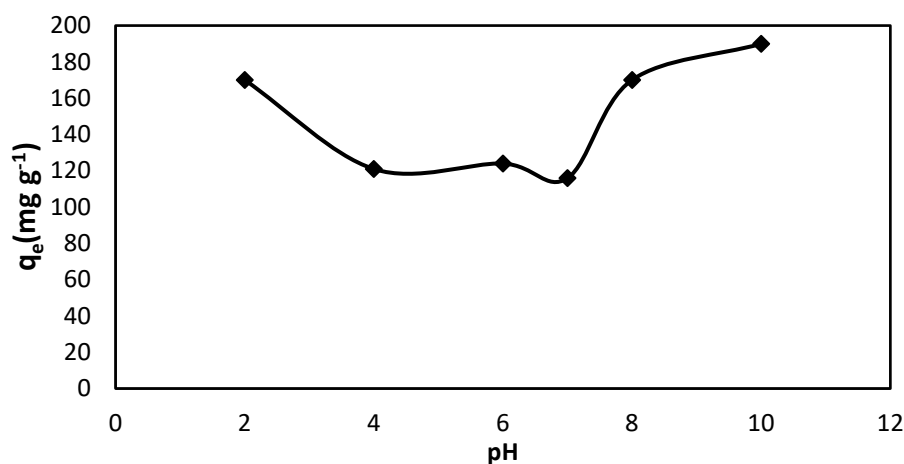


Fig. 3d. Outcome of pH on BG

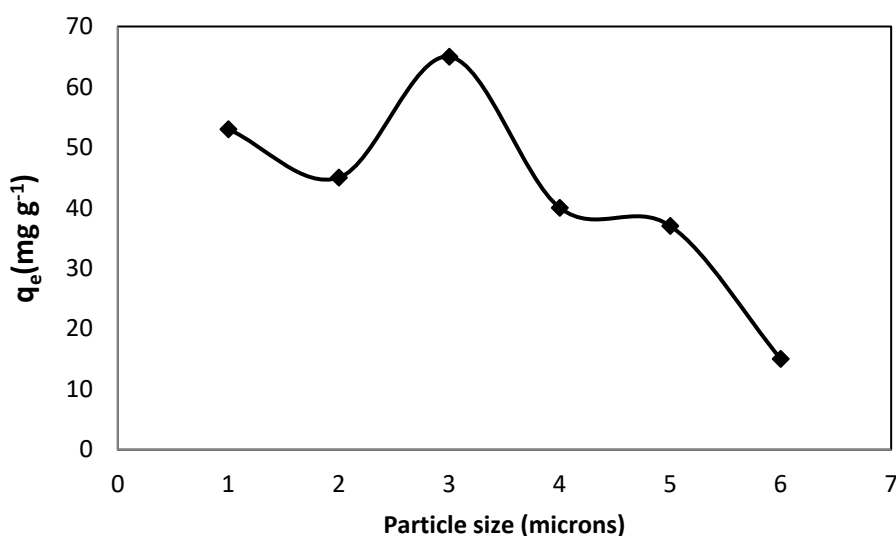


Fig. 3e. Outcome of particle size

3.3. Adsorption isotherms

Adsorption isotherms provide crucial insights into the equilibrium between the adsorbent material and the adsorbate when temperature, pressure, and concentration are constant. They clarify the exchanges between adsorbate molecules and the adsorbent's surface. This work inspected the adsorption of BG onto NIFSS using various adsorption isotherm models.

The Langmuir model suggests monolayer adsorption on the adsorbent's surface based on the notion that there is a fixed sum of identical adsorption spots with a homogeneous amount of energy (Langmuir 1916). This study shows R_L values of 0.222 to 0.774, representing favourable BG adsorption to NIFSS. The fact that R_L falls off as the initial concentration rises demonstrates that adsorption is more advantageous at upper concentrations. The significant discrepancy between Q_m 227.8 mg g⁻¹ and q_e 150 mg g⁻¹ suggests the need to investigate further adsorption isotherm models.

The empirical Freundlich isotherm model agrees that adsorption is heterogeneous (Freundlich 1906). In this study, n_F was found to be 1.831, and $1/n_F$ was 0.546, suggesting that adsorption is physisorption, favouring a typical Langmuir Isotherm.

Overall, the Langmuir and Freundlich isotherms exhibited correlation coefficients (R^2) of 0.99 and 0.94, respectively, indicating a linear process. Under the investigational circumstances, it was determined that the adsorption of BG onto NIFSS was favourable and was primarily characterised as physisorption.

In summary, the study provides valuable insights into the favourable adsorption behaviour of BG onto NIFSS, indicating that it is largely physisorption as determined by the Langmuir and Freundlich isotherm models.

The Jovanovic isotherm, an extended method of the Langmuir isotherm (Jovanović 1969), posits a monolayer adsorption process with no lateral interactions. An additional exponential term is introduced in this model to account for deviations observed in experimental results from the Langmuir isotherm. Notably, the maximum adsorption capacity (Q_m) designed from the Jovanovic isotherm (163.38 mg g^{-1}) is nearer to q_e value.

On the other hand, the Dubinin-Radushkevich isotherm (Dubinin 1947), an empirical model that was first developed for pore-filling-based adsorption processes, produces a Q_s value of 136.17 mg g^{-1} , which is less than the observed value. The Dubinin-Radushkevich isotherm, despite this disagreement, showed a satisfactory match to the trial data with an R^2 value of 0.94, indicating a linear relationship. In summary, the Jovanovic isotherm, an extension of the Langmuir model, offers a healthier fit to the trial records by incorporating an additional exponential term. The Dubinin-Radushkevich isotherm, while yielding a lower Q_s value, also demonstrates a linear relationship with the experimental data.

In summary, the investigation involved three complementary two-parameter models: Langmuir, Freundlich, Jovanovic, and Dubinin-Radushkevich, with results presented in Table 1 and Fig. 4a. These models collectively imply that the relationship between BG and NIFSS is linear, advantageous, and physical. Notably, Jovanovic offers a better fit, particularly in terms of Q_m , the maximum adsorption capacity, compared to the other three models.

For academic exploration, six three-parameter isotherm models were also examined. The Sips isotherm (Sips 1948) combines elements of both Langmuir and Freundlich isotherms. The Freundlich equation describes low adsorbate deliberations and high adsorbate concentrations are characterised by an approach to the Langmuir isotherm, as shown in Fig. 4b. The 'g' value of 1.482 found in this investigation indicates that the adsorption is more likely to follow the Langmuir isotherm (Redlich & Peterson 1969). The Toth isotherm (Toth 1971) is another realistic comparison designed to rally the fitting of the Langmuir isotherm and label the heterogeneous adsorption systems. As indicated in Table 2 and Fig. 4c, the Q_m value of 164.5 mg g^{-1} closely approximates the experimental q_e value of 150 mg g^{-1} , in contrast to the Langmuir isotherm rate of 227.8 mg g^{-1} .

Overall, this comprehensive analysis provides insights into BG's adsorption behaviour on NIFSS, with various isotherm models shedding light on different aspects of the adsorption process.

The Vieth-Sladek isotherm model (Vieth & Sladek 1965) was initially used to describe solutes that were undergoing following particular adsorption following a particular isotherm that incorporated both a non-linear (Langmuir equation) and a linear (Henry's law) component. The non-linear component denotes solute adhesion to locations on the exterior of permeable adsorbents, whereas the linear component indicates solute dissolution in the amorphous portions of adsorbent polymers. This model predicts the highest Q_m value among the models examined, 227.7 mg g^{-1} . Transient adsorption is used to estimate diffusion rates within solid materials using the Vieth-Sladek isotherm model.

The Brouers-Sotolongo isotherm (Brouers et al. 2005) shares similarities with the Vieth-Sladek isotherm. It employs a mathematical equation comprising the K_{BS} and α variable, describing the adsorbent-adsorbate system's active site circulation and adsorption capacity. The Q_m value attained for this isotherm is 154.5 mg g^{-1} , which closely approximates the investigational value of q_m (188 mg g^{-1}). Moreover, the high R^2 value of 0.99 indicates a good match of the investigational data to this isotherm, as shown in Fig. 4d.

The Radke-Prausnitz isotherm model (Radke & Prausnitz 1972) appears to be well-suited for describing the BG-NIFSS system, as it yields the maximum Q_m value and demonstrates a good χ^2 value of 1.664.

In summary, these various isotherm models, including Vieth-Sladek, Brouers-Sotolongo, and Radke-Prausnitz, contribute to a comprehensive understanding of the adsorption process between BG and NIFSS. Each model provides valuable insights into different aspects of the adsorption behaviour.

In short, among all the models, both the Jovanovich and Brouers-Sotolongo models yield adsorption capacities very near the investigational q_e value of 150 mg g^{-1} . These two models demonstrate a better fit compared to the others.

In conclusion, the models utilised to comprehend the adsorption mechanism use higher-order equations. In isolation, the R^2 value – only applicable to linear models – cannot be used to assess the quality of data fitting. Therefore, χ^2 values are also reflected, as they offer a more robust statistical assessment. A small χ^2 value designates that the model data closely resemble the investigational data, while a larger value suggests the opposite. All nine isotherm models provided parameter values (Q_m , χ^2 , and R^2) as presented in Table 3. The scientific community, especially mathematical modelling specialists, finds all models and the experimental values (q_e) fascinating and may explore developing new models to enhance our understanding of the adsorption process in the BG-NIFSS system.

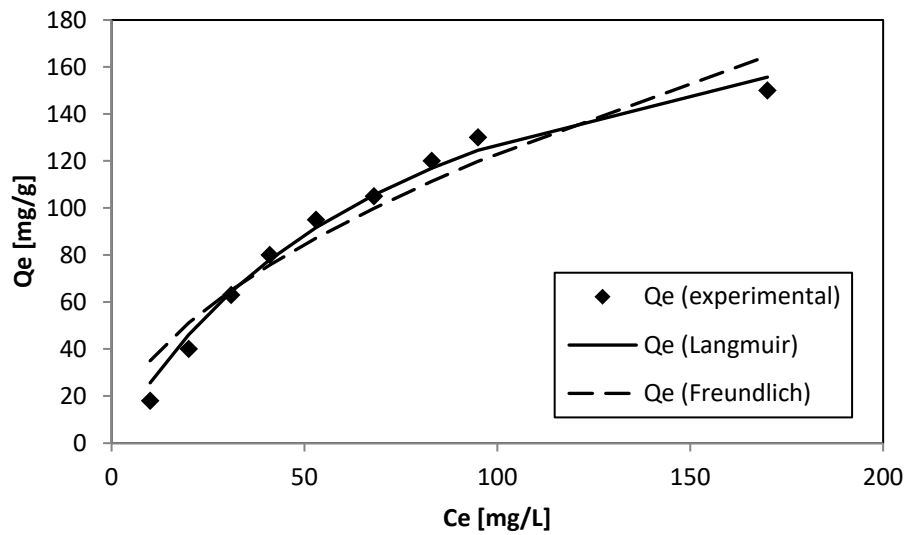


Fig. 4a. Langmuir and Freundlich adsorption isotherm

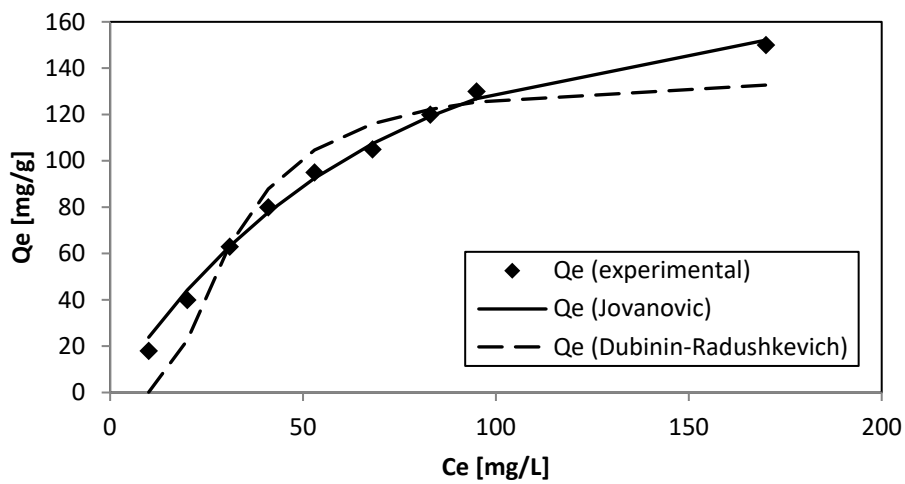


Fig. 4b. Jovanovic and Dubinin-Radushkevich adsorption isotherm

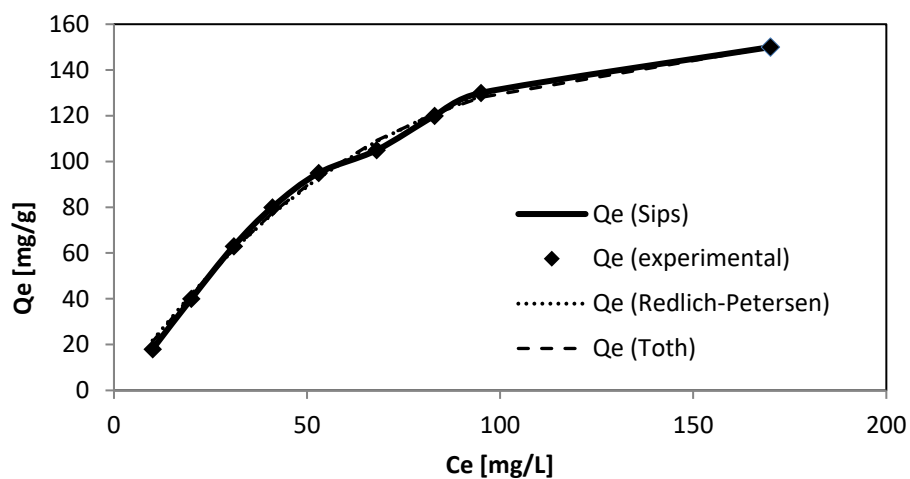


Fig. 4c. Sips, Redlich-Petersen and Toth adsorption isotherm

3.4. Adsorption kinetics

The kinetic studies were conducted at 50, 100, and 200 ppm BG concentrations, a methodology in line with previous studies (Hameed & El-Khaiary 2008, Ahmad & Kumar 2010). Examining kinetics at unlike temperatures (303 K, 313 K, and 323 K) allowed us to observe variations in the adsorption rate under different temperature conditions. These adsorption kinetics were assessed through non-linear analyses using various models, including the pseudo-first-order model (Largegren 1898), pseudo-second-order model (Ho & McKay 1998), intra-particle diffusion via the Weber-Morris model (Alkan et al. 2007), the Dumwald-Wagner model (Wang et al. 2004), and the Film Diffusion model (Boyd et al. 1947).

For all initial BG concentrations of 50, 100, and 200 ppm, the pseudo-second-order model revealed a healthier fit with the trial documents founded on the factors of purpose (R^2) and chi-square values (χ^2) (as shown in Figs. 5a, 5b, and 5c). After obtaining maximum adsorption, the adsorption rate steadily drops until it reaches a constant level. In addition, as the temperature rose, the adsorption capacity (q_e) increased (see Table 4). These results demonstrated the non-rate-limiting nature of the adsorption processes.

During the adsorption process, the solute molecules transfer from the solution to the solid surface, subsequently diffusing into the NIFSS's pores. The data were analysed to look into the impacts of diffusion and learn more about the movement of solutes.

The Dumwald-Wagner model (seen in Fig. 5d) was applied to determine the real absorption rate constant (K) while considering detected diffusion possessions. The Weber-Morris model (depicted in Fig. 5e) links solute approval to $t^{1/2}$ rather than the time of contact (t), and explains molecular diffusion. Multiple mechanisms often govern adsorption kinetics. In our experimental data, we observe various levels of linearity at all solute concentrations. The adsorption rate is initially great and follows a divergent linear trajectory before eventually stabilising over time at lesser initial concentrations (50 ppm) and lesser temperatures. The larger temperatures cause the rate to behave almost linearly, whereas larger solute concentrations (>200 ppm) do not significantly alter the adsorption rate. When applying the liquid film diffusion model to the upper-temperature data, this pattern becomes especially clear (Boyd et al. 1947), as shown in Fig. 5f. This model fits well with high R^2 and χ^2 values and provides a diffusion constant R^1 . Diffusion constraints barely affect the adsorption rate at higher temperatures. Diffusion is, hence, the rate-limiting process, it might be said. The solute first quickly forms a coating on the particle surfaces, preventing further diffusion. This elucidates the noticeable variations in absorption rates. The results are summarised in Table 5.

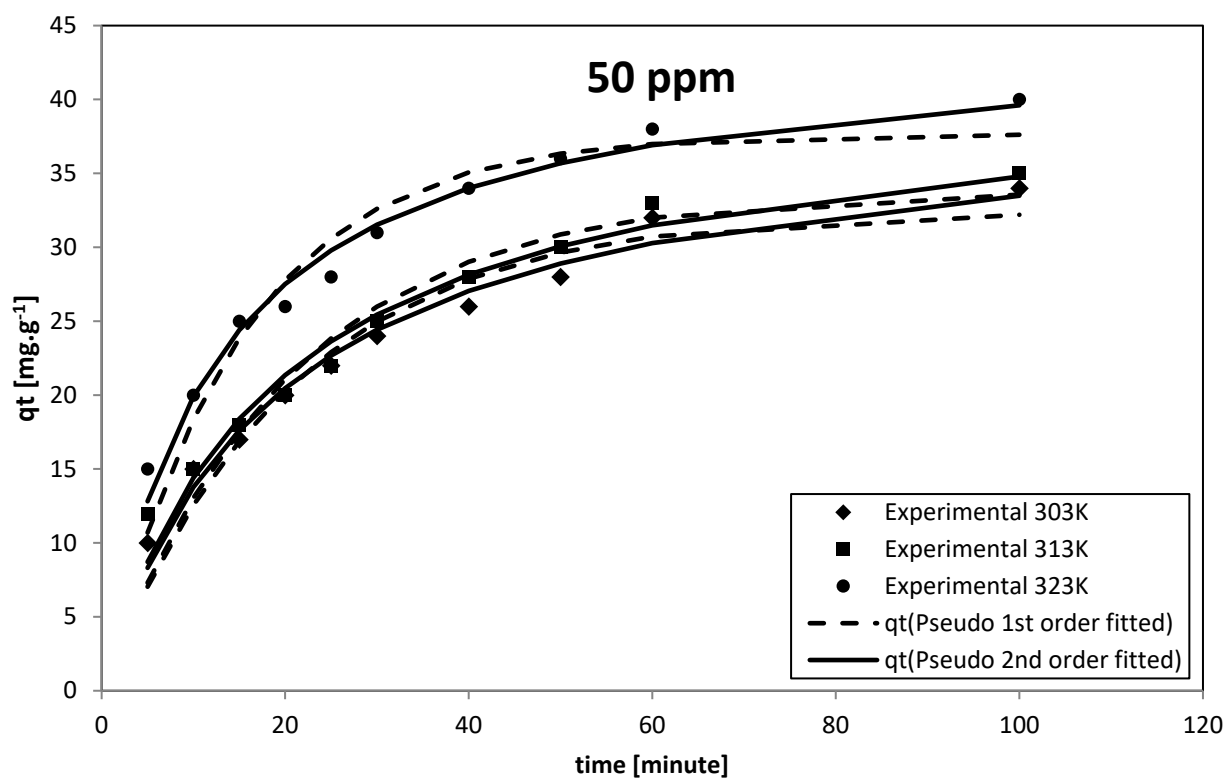


Fig. 5a. 50 ppm Kinetic model

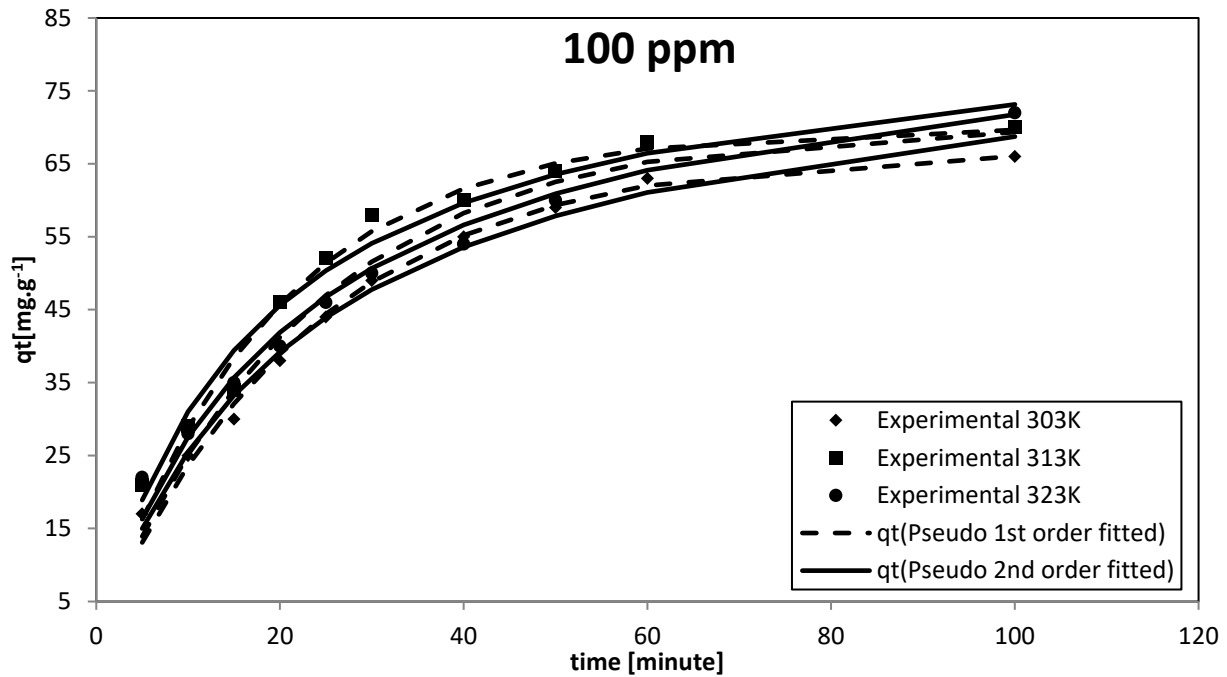


Fig. 5b. 100 ppm Kinetic model

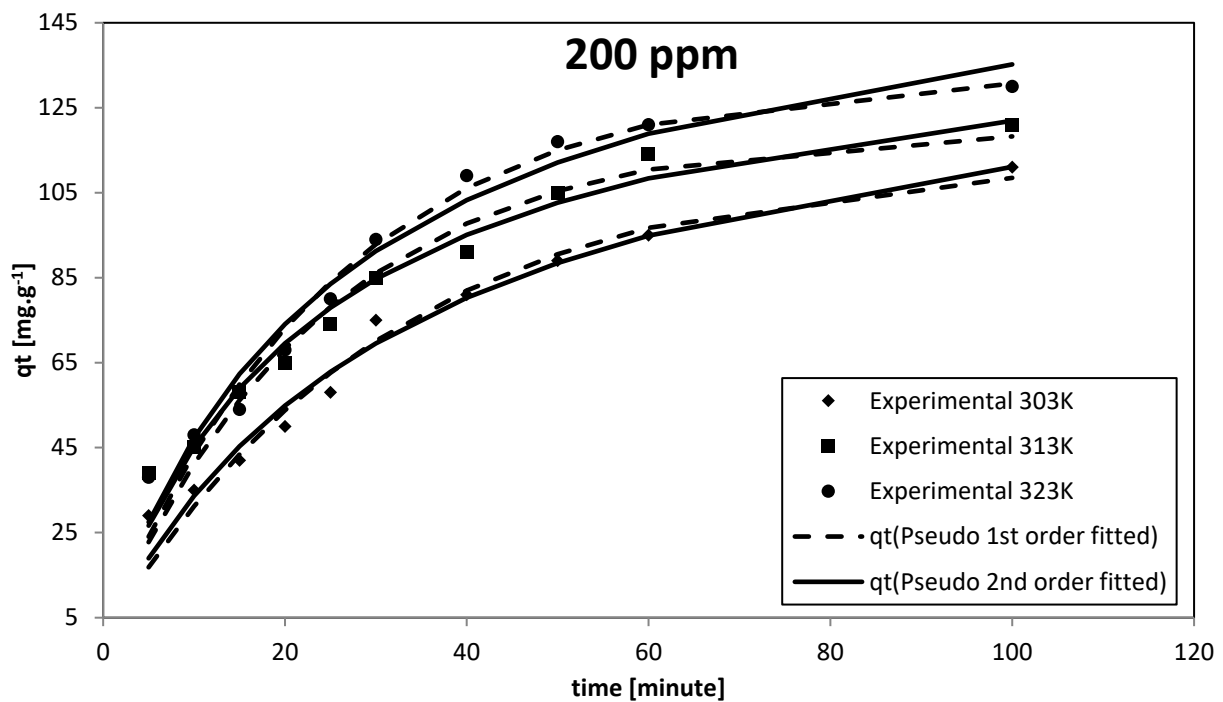


Fig. 5c. 200 ppm Kinetic model

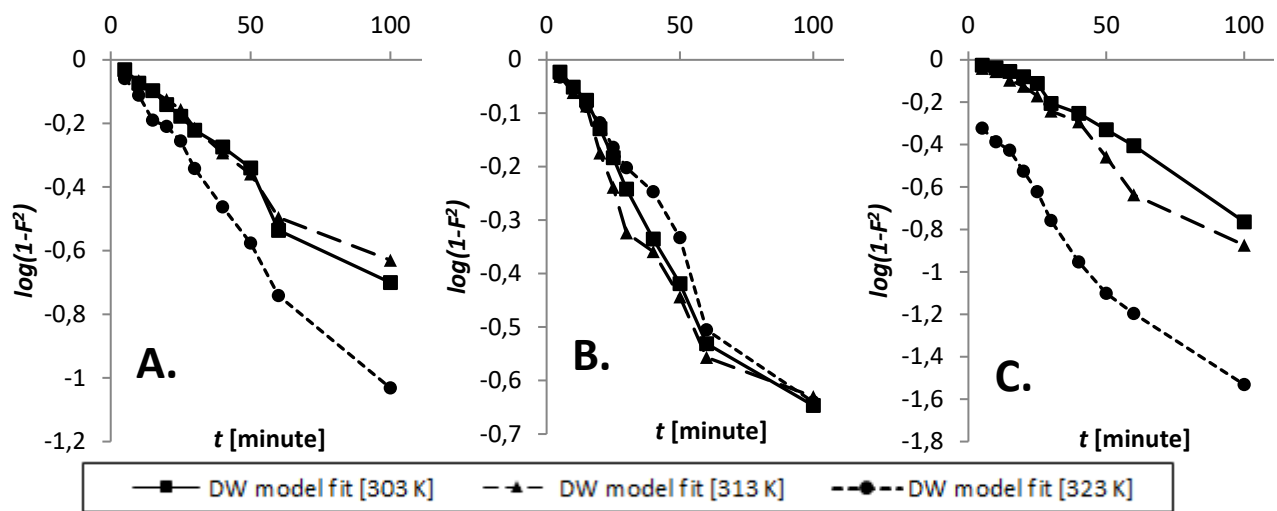


Fig. 5d. Kinetics data of BG: A) 50 ppm, B) 100 ppm, C) 200 ppm

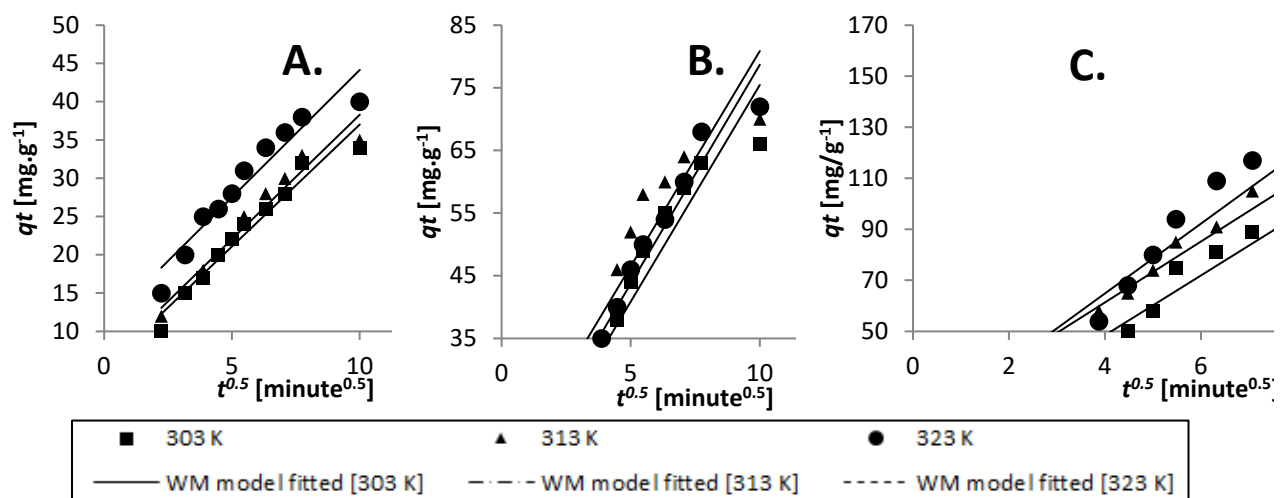


Fig. 5e. Kinetics data of BG: A) 50 ppm, B) 100 ppm, C) 200 ppm

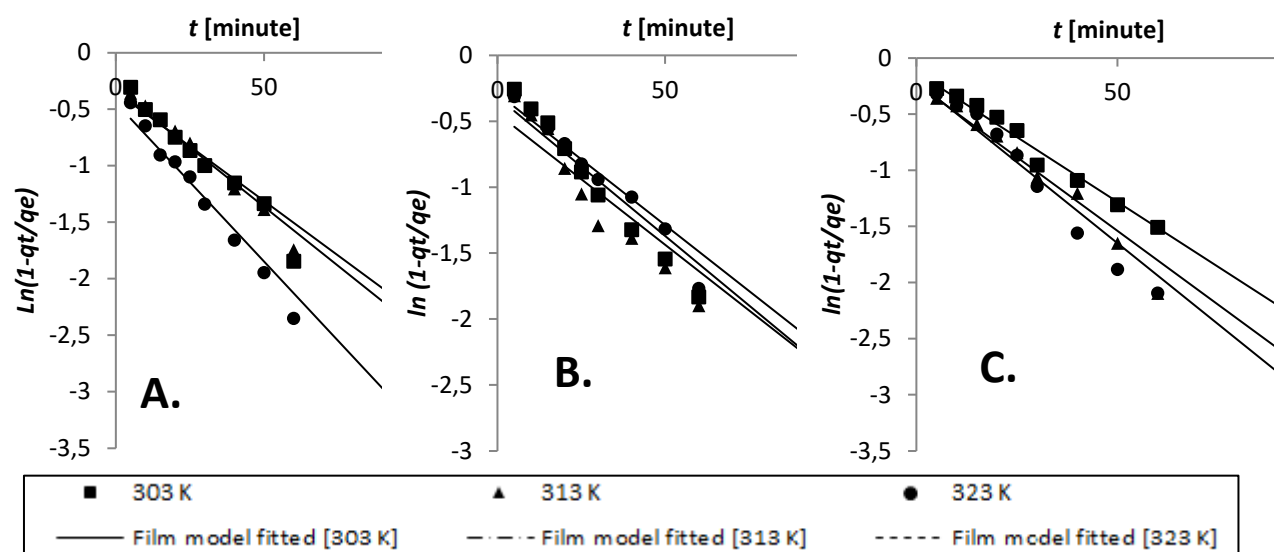


Fig. 5f. Kinetics data of BG: A) 50 ppm, B) 100 ppm, C) 200 ppm

Table 4. Parameters for models of absorption kinetics that have been experimentally determined and predicted

Initial Concentration	Temp	$Q_{e,exp}$ [mg.g ⁻¹]	Pseudo First order				Pseudo Second order			
			$Q_{e,pred}$ [mg.g ⁻¹]	k_1	R ²	χ^2	$Q_{e,pred}$ [mg.g ⁻¹]	k_2	R ²	χ^2
[ppm]	[K]									
50	303	38	32.45	4.89E-02	0.96	1.73	39.84	1.33E-03	0.98	1.73
	313	40	33.82	4.87E-02	0.96	2.49	41.29	1.30E-03	0.97	1.22
	323	42	37.67	6.68E-02	0.95	2.07	44.51	1.82E-03	0.98	0.58
100	303	75	66.92	4.35E-02	0.99	1.16	84.71	5.08E-04	0.99	0.90
	313	80	70.00	7.00E+01	0.98	1.79	65.88	1.71E-03	0.76	1.65
	323	82	70.20	4.42E-02	0.97	4.04	87.34	5.27E-04	0.98	1.94
200	303	122	112.96	3.23E-02	0.97	6.64	149.32	1.95E-04	0.97	5.09
	313	130	120.07	4.21E-02	0.97	8.21	150.29	2.87E-04	0.97	4.99
	323	138	133.24	3.98E-02	0.97	6.86	170.41	2.26E-04	0.97	5.74

Table 5. Calculated parameters for diffusion models

Initial Concentration	Temp	Film diffusion model		Weber-Morris model		Dumwald-Wagner	
		R ¹ [min ⁻¹]	R ²	k_{ist} [mg g ⁻¹ s ^{-0.5}]	R ²	K [min ⁻¹]	R ²
[ppm]	[K]						
50	303	0.0210	0.96	3.19	0.95	0.017	0.97
	313	0.0194	0.95	3.25	0.95	0.015	0.97
	323	0.0281	0.97	3.33	0.92	0.025	0.98
100	303	0.0211	0.92	6.92	0.91	0.017	0.94
	313	0.0199	0.87	6.87	0.87	0.016	0.89
	323	0.0200	0.96	6.99	0.96	0.016	0.96
200	303	0.0231	0.99	11.72	0.96	0.018	0.99
	313	0.0263	0.97	11.94	0.95	0.022	0.97
	323	0.0288	0.96	13.67	0.92	0.032	0.95

3.5. Effect of adsorption thermodynamics

The standard enthalpy alteration for a typical chemical reaction is >200 kJ mol⁻¹; the positive values of ΔH° show that the adsorption method is endothermic and, therefore, physical in this instance. Additionally, as temperature rises, the adsorption capacity rises as well. The positive value of S_o shows increased randomisation at the solid solution's surface, which also shows that BG has a significant affinity for the adsorbent.

The negative G_o values, which show a decline in Gibbs free energy, confirm the viability and spontaneity of the adsorption process. The ΔG° value is negative for all temperatures, demonstrating that the adsorption of BG onto NIFSS proceeds naturally and advantageously. Interestingly, the ΔG° value lowers as the temperature rises, indicating a greater adsorption capability. Table 6 provides a summary of the thermodynamic variables.

Table 6. Calculated thermodynamic parameters

Concentration (mg L ⁻¹)	ΔH^0 (kJ mol ⁻¹)	ΔS^0 (J mol ⁻¹ K ⁻¹)	ΔG^0 (kJ mol ⁻¹)		
			303 K	313 K	323 K
50	20.45	90.27	6.92	7.82	8.70
100	17.07	79.03	6.86	7.65	8.44
150	15.70	69.11	5.23	5.92	6.16
200	14.27	64.16	5.16	5.80	6.44

3.6. Cost analysis and adsorbent regeneration

Due to the high process cost and associated solvent costs, which would probably exceed the cost of the sorbents utilised in the method, it is not recommended to regenerate dye-loaded NIFSS for reuse and recovery of the adsorbed material. Additionally, this strategy would result in an unwanted rise in the E-factor as it would contribute to a greater environmental load of toxic substances. An alternative and more beneficial approach would involve repurposing waste process materials, such as the ongoing development of methods to produce thermosets and thermoplastics.

4. Conclusion

The first-ever study focused on utilising fennel seed spent, a Nutraceutical Industrial Spent was made to progress an efficient and environmentally friendly biosorbent to eliminate the hazardous colour brilliant green. The study revealed that the maximum adsorption capacity is closely aligned with the Brouers-Sotolongo model, with the highest fitting isotherm achieved using the Redlich-Peterson model. The experimental data fitted to the kinetic model of pseudo-second order, which the Avrami kinetic model further validated. Additionally, significant effects of film and intra-particle diffusion were observed in the adsorption method. The adsorption process was determined to be spontaneous and endothermic, with a low ΔH^0 value specifying a predominantly physical mechanism. FTIR spectra confirmed the adsorption of brilliant green on NIFSS.

In conclusion, NIFSS is an adsorbent for the quick and current elimination of brilliant green from aqueous solutions. It is potentially used in alternative structural materials or as fillers to produce thermoplastics and thermosets.

Statements and Declarations

Acknowledgment

The authors extend their appreciation to the Deanship of Research and Graduate Studies at King Khalid University for funding this work through Large Research Project under grant number RGP2/324/45.

Disclosure Statement

All authors declare no conflict of interest.

References

- Ahmad, R., Kumar, R. (2010). Adsorption studies of hazardous malachite green onto treated ginger waste. *Journal of Environmental Management*, 91(4), 1032-1038.
- Alkan, M., Demirbaş, Ö., Doğan, M. (2007). Adsorption kinetics and thermodynamics of an anionic dye onto sepiolite. *Microporous and Mesoporous Materials*, 101(3), 388-396.
- Boyd, G.E., Adamson, A.W., Myers, JR, L.S. (1947). The exchange adsorption of ions from aqueous solutions by organic zeolites. II. kinetics. *Journal of the American Chemical Society*, 69(11), 2836-2848.
- Asadullah, M., Asaduzzaman, M., Kabir, M.S., Mostofa, M.G., Miyazawa, T. (2010). Chemical and structural evaluation of activated carbon prepared from jute sticks for Brilliant Green dye removal from aqueous solution. *Journal of Hazardous Materials*, 174(1-3), 437-443.
- Bhattacharyya, K.G., Sarma, A. (2003). Adsorption characteristics of the dye, Brilliant Green, on Neem leaf powder. *Dyes and Pigments*, 57(3), 211-222.
- Brouers, F., Sotolongo, O., Marquez, F., Pirard, J.P. (2005). Microporous and heterogeneous surface adsorption isotherms arising from Levy distributions. *Physica A: Statistical Mechanics and its Applications*, 349(1), 271-282.
- Dubinin, M.M. (1947). The equation of the characteristic curve of activated charcoal. In *Dokl Akad Nauk SSSR*, 55, 327-329.
- Filipkowska, U., Klimiuk, E., Grabowski, S., Siedlecka, E. (2002). Adsorption of reactive dyes by modified chitin from aqueous solutions. *Polish Journal of Environmental Studies*, 11(4), 315-324.
- Freundlich, H.M.F. (1906). Over the adsorption in solution. *Journal of Physical Chemistry*, 57(385471), 1100-1107.

- Gupta, T., Ansari, K., Lataye, D., Kadu, M., Khan, M. A., Mubarak, N. M., ... & Karri, R. R. (2022). Adsorption of Indigo Carmine Dye by *Acacia nilotica* sawdust activated carbon in fixed bed column. *Scientific Reports*, *12*(1), 15522.
- Garg, V.K., Gupta, R., Yadav, A.B., Kumar, R. (2003). Dye removal from aqueous solution by adsorption on treated sawdust. *Bioresource Technology*, *89*(2), 121-124.
- Hameed, B.H., El-Khairi, M.I. (2008). Malachite green adsorption by rattan saw dust: Isotherm, kinetic and mechanism modeling. *Journal of Hazardous Materials*, *159*(2), 574-579.
- Haris, M.R., Sathasivam, K. (2009). The removal of methyl red from aqueous solutions using banana pseudostem fibers. *American Journal of Applied Sciences*, *6*(9), 1690.
- Hiroyuki, H., Hideki, N., Kataoka, T. (1994). Adsorption of BSA on strongly basic chitosan–equilibria. *Biotechnology and Bioengineering*, *43*, 1087-1093.
- Ho, Y.S., McKay, G. (1998). Sorption of dye from aqueous solution by peat. *Chemical Engineering Journal*, *70*(2), 115-124.
- Jovanović, D.S. (1969). Physical adsorption of gases. *Kolloid-Zeitschrift und Zeitschrift für Polymere*, *235*(1), 1203-1213.
- Kadirvelu, K., Kavipriya, M., Karthika, C., Radhika, M., Vennilamani, N., Pattabhi, S. (2003). Utilisation of various agricultural wastes for activated carbon preparation and application for the removal of dyes and metal ions from aqueous solutions. *Bioresource Technology*, *87*(1), 129-132.
- Lagergren, S. (1898). About the theory of so-called adsorption of soluble substances. *Kungliga Svenska Vetenskapsakademiens Handlingar*, *24*, 1-39.
- Langmuir, I. (1916). The constitution and fundamental properties of solids and liquids. *Journal of the American Chemical Society*, *38*(11), 2221-2295.
- Mane, V.S., Mall, I.D., Srivastava, V.C. (2007). Kinetic and equilibrium isotherm studies for the adsorptive removal of Brilliant Green dye from aqueous solution by rice husk ash. *Journal of Environmental Management*, *84*(4), 390-400.
- Mittal, A., Kaur, D., Mittal, J. (2008). Applicability of waste materials – bottom ash and deoiled soya – as adsorbents for the removal and recovery of a hazardous dye, brilliant green. *Journal of Colloid and Interface Science*, *326*(1), 8-17.
- Namasivayam, C., Radhika, R., Suba, S. (2001). Uptake of dyes by a promising locally available agricultural solid waste: coir pith. *Waste Management*, *21*(4), 381-387.
- Nandi, B.K., Goswami, A., Purkait, M.K. (2009). Removal of cationic dyes from aqueous solutions by kaolin: kinetic and equilibrium studies. *Applied Clay Science*, *42*(3-4), 583-590.
- Nandi, B.K., Goswami, A., Purkait, M.K. (2009a). Adsorption characteristics of brilliant green dye on kaolin. *Journal of Hazardous Materials*, *161*(1), 387-395.
- Radke, C.J., Prausnitz, J.M. (1972). Thermodynamics of Multi-Solute Adsorption from Dilute Liquid Solutions. *Alche Journal*, *18*, 761-768.
- Redlich, O., Peterson, D.L. (1969) A useful adsorption isotherm. *Journal of Physical Chemistry*, *63*, 1024-1026.
- Salman, J.M., Hameed, B.H. (2010). Adsorption of 2, 4-dichlorophenoxyacetic acid and carbofuran pesticides onto granular activated carbon. *Desalination*, *256*(1-3), 129-135.
- Sheldon, R.A. (1992). Organic synthesis-past, present and future. *Chemistry and Industry*, (23), 903-6.
- Sips, R. (1948). Combined form of Langmuir and Freundlich equations. *Journal of Physical Chemistry*, *16*(429), 490-495.
- Sudamalla, P., Pichiah, S., Manickam, M. (2012). Responses of surface modeling and optimisation of Brilliant Green adsorption by adsorbent prepared from Citrus limetta peel. *Desalination and Water Treatment*, *50*(1-3), 367-375.
- Toth, J. (1971). State equations of the solid gas interface layer. *Acta Chem Acad Hungary*, *69*, 311-317.
- Vieth, W.R., Sladek, K.J. (1965). A model for diffusion in a glassy polymer. *Journal of Colloid Science*, *20*(9), 1014-1033.
- Wang, H.L., Chen, J.L., Zhai, Z.C. (2004). Study on thermodynamics and kinetics of adsorption of p-toluidine from aqueous solution by hypercrosslinked polymeric adsorbents. *Environmental Chemistry*, *23*(2), 188-192.
- Wang, S., Li, H., Xie, S., Liu, S., Xu, L. (2006). Physical and chemical regeneration of zeolitic adsorbents for dye removal in wastewater treatment. *Chemosphere*, *65*(1), 82-87.
- Waghmare, C., Ghodmare, S. D., Ansari, & K. A. (2023). Experimental investigation of H₃PO₄ activated papaya peels for methylene blue dye removal from aqueous solution: Evaluation on optimization, kinetics, isotherm, thermodynamics, and reusability studies. *Journal of Environmental Management*, *345*, 118815.
<https://doi.org/10.1016/j.jenvman.2023.118815>
- Waghmare, C., Ghodmare, S., Ansari, K., Alfaisal, F. M., Alam, S., Khan, M. A., & Ezaier, Y. (2024). Adsorption of methylene blue dye onto phosphoric acid-treated pomegranate peel adsorbent: Kinetic and thermodynamic studies. *Desalination and Water Treatment*, 100406.
- Webber, T.W., Chakravorti, R.K. (1974). Pore and solid diffusion models for fixed-bed adsorbents. *Alche Journal*, *20*(2), 228-238.
- Zollinger, H. (2002). Synthesis, properties and applications of organic dyes and pigments. Colour chemistry.
<https://www.ibef.org/>
<http://www.spices.res.in/spices/fennel.php>